

Satellite-detected chlorophyll fluorescence reveals physiology and photosynthetic pigments of global ocean phytoplankton

Michael J. Behrenfeld, Toby Westberry, Emmanuel Boss, Robert O'Malley, Jerry Wiggert, David Siegel, Bryan Franz, Chuck McClain, Gene Feldman, Giorgio Dall'Omo, Allen Milligan, Scott Doney, Ivan Lima, Natalie Mahowald

Overview

MODIS fluorescence data were used to evaluate global chlorophyll products and investigate physiological properties of phytoplankton

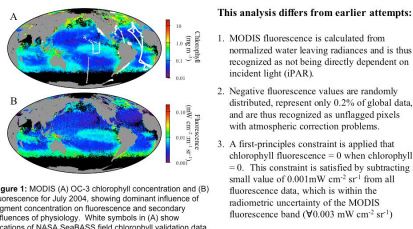


Figure 1: MODIS (A) OC-3 chlorophyll concentration and (B) fluorescence for July 2004, showing dominant influence of pigment concentration on fluorescence and secondary influences of physiology. White symbols in (A) show locations of NASA SeaWiFS field chlorophyll variation data.

Conclusions

- When compared to fluorescence data, bio-optical chlorophyll algorithms (QAA, GSM) outperform traditional wavelength ratio algorithms (OC-3) in the clearest ocean waters, while in more productive regions OC-3 outperforms QAA and GSM
- The relationship between fluorescence and chlorophyll is clearly influenced by pigment packaging effects, which can be accounted for using published coefficients
- The primary physiological contribution to fluorescence variability is nonphotochemical quenching, which can be described to first-order as an inverse function of light (i.e., $1/\text{IPAR}$)
- Iron stress effects are a secondary, but clear contributor to variability in fluorescence yields and reflect changes in photosystem stoichiometry (i.e., PSII:PSI ratios)
- Photoacclimation is also a second-order influence on fluorescence yields that functions through altering nonphotochemical quenching relationships with IPAR

Fluorescence & Chlorophyll

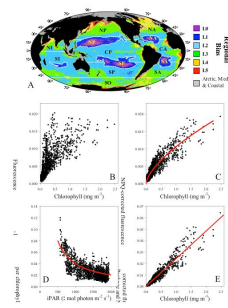


Figure 3A: To illustrate the primary dependencies of fluorescence, monthly MODIS data for the 5-year record (2002-2007) were separated into 34 regional bins based on ocean basin and seasonal variability in chlorophyll. NP, CP, SP = north, central, and south Pacific, respectively. NA, CA, SA = north, central, and south Atlantic. NI, SI = north and south Indian. SO = Southern Ocean. Colors indicate increasing seasonal chlorophyll variability from lowest (purple) to highest (red) (color bar on right). Coastal and Arctic data are not included in this analysis (gray areas). The 34 bins represent 95% of the global open ocean area.

Figure 3B: Relationship between binned fluorescence ($\text{mW cm}^{-2} \text{ sr}^{-1}$) and OC-3 chlorophyll (mg m^{-3}) data, showing dominant effect of pigment variability on fluorescence as in Figure 1.

Figure 3C: Effects of pigment packaging are best seen by comparing chlorophyll with NPQ-corrected fluorescence. Red line = relationship between chlorophyll concentration and light absorption (relative) based on change in pigment packaging (α^*) for the primary absorption band for photosynthesis (400-530 nm) from Bricaud et al. (1998).

Figure 3D: Effects of NPQ are best seen by comparing package-corrected fluorescence per unit chlorophyll with IPAR. Red line = $1/\text{IPAR}$ (relative).

Figure 3E: Relationship between OC-3 chlorophyll and fluorescence corrected for NPQ and pigment packaging ($r = 0.96$)

Fluorescence & Iron Stress

The NPQ-corrected quantum yield of fluorescence (f_{NPQ}) registers physiological responses to a wide range of environmental factors, with iron stress being prominent. The reason iron-stress influences quantum yields is that *in vivo* fluorescence emanates almost entirely from PSII, while chlorophyll (thus, absorption) is a product of both PSII and PSI pigments. Division of fluorescence by absorption consequently gives quantum yields that are sensitive to PSII:PSI ratios, which are strongly influenced by iron availability.

Global comparisons of fluorescence quantum yields with aeolian dust deposition illustrates that elevated fluorescence yields are correlated with low iron conditions. However, some low-iron regions do not have high quantum yields (e.g., subarctic north Pacific) because of compensating effects of low-light photoacclimation (Fig. 2C).

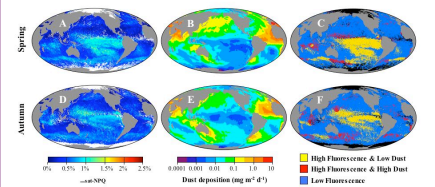


Figure 6: Comparison of (A,D) NPQ-corrected fluorescence quantum yields (f_{NPQ}) and (B,E) aeolian dust deposition. (C,F) State-space comparison of f_{NPQ} and dust deposition. Yellow pixels indicate high f_{NPQ} ($>0.7\%$ relative units) and low dust ($<0.02 \text{ mg m}^{-2} \text{ d}^{-1}$). (A-C) Spring (March-May). (D-F) Autumn (September-November). Spring and Autumn are shown because the latitudinal distribution of light is most evenly distributed across mid- and low-latitudes during these seasons, thus minimizing impacts of photoacclimation.

Fluorescence Basics

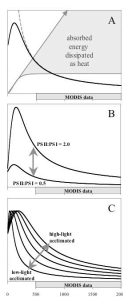


Figure 2A: Light absorption is a linear function of incident light (IPAR, $\text{umol photons m}^{-2} \text{ s}^{-1}$) (light gray arrow). Photosynthesis saturates at a relatively low light level (in this case, $150 \text{ umol photons m}^{-2} \text{ s}^{-1}$) (curved gray line). The difference between absorbed light and that used for photosynthesis is dissipated as heat (NPQ) (shaded gray area). Fluorescence per unit absorbed light energy initially increases as photosynthesis saturates, then decreases as a greater fraction of absorbed energy is dissipated as heat (NPQ) (black line). Shortly after saturation, this decrease in fluorescence yield approximates a $1/\text{IPAR}$ relationship (dashed gray line).

Figure 2B: Iron stress affects PSII:PSI ratios. A change in PSII:PSI from 0.5 (lower curve) to 2.0 (upper curve) causes a proportional change in fluorescence yields.

Figure 2C: Photosynthesis in lower light acclimated cells saturates at lower light levels, so NPQ is more severe (lower curves) when exposed to a high IPAR than for a high-light acclimated cells (upper curves).

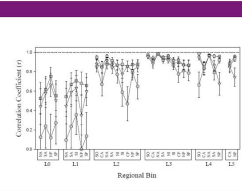
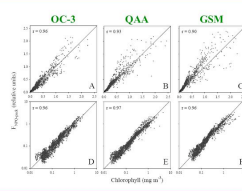
ALL FIGURES: MODIS measurements are always made under supersaturating light conditions when NPQ is strongly expressed and follows an inverse function of IPAR. Gray bar in each panel indicates IPAR range for MODIS (500 to 2100 $\text{umol photon m}^{-2} \text{ s}^{-1}$)

Chlorophyll Algorithms

NPQ- and package-corrected fluorescence data were compared to chlorophyll estimates from the empirical OC-3 algorithm and two bio-optical algorithms (QAA, GSM).

Figure 4A-C: On linear axes, it is clear that the OC-3 estimates agree best with fluorescence at high chlorophyll concentrations

Figure 4D-F: On log-transformed axes, advantages of the bio-optical algorithms are more apparent in low chlorophyll waters



Regional Performance

Figure 5: Correlation coefficients (r) and 95% confidence intervals for regional relationships between NPQ- and package-corrected fluorescence and chlorophyll for the three chlorophyll algorithms. Circles = OC-3. Squares = QAA. Triangles = GSM. Data are sorted by variance bins (see Fig. 3A) from low variance (L0) on left going to high variance (L5) on right. Basin designations are shown along the x-axis

Iron Stress & the Indian Ocean

One of the most prominent global features in fluorescence quantum yields (f_{NPQ}) is a band of enhanced values found each summer (June – August) in the central Indian Ocean that stretches nearly the width of the basin and extends northward along the western boundary. This feature corresponds to minima in dust deposition and the predicted occurrence of iron-stressed surface phytoplankton based on an ocean circulation ecosystem model (Wiggert et al. 2006), again emphasizing the role of iron in satellite fluorescence data and representing the first basin-scale observational evidence supporting anticipated iron stress in this region.

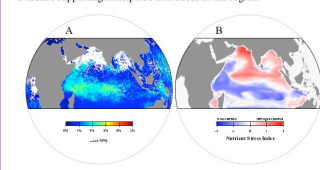


Figure 7: (A) Summer NPQ-corrected fluorescence quantum yields (f_{NPQ}). (B) Summer model estimates of the most limiting nutrient (nitrogen or iron) for surface phytoplankton (Wiggert et al. 2006). Red = tendency for N limitation. Blue = tendency for Fe limitation.

Citation: Wiggert, J., R.Murtugudde, J.Christian. 2006. Deep-Sea Res. II 53, 644-676.

